Extremum Co-Energy Principle for Analyzing AC Current Distribution in Parallel-Connected Wires of High Frequency Power Inductors

T. Shirakawa*, G. Yamasaki*, K. Umetani*, and E. Hiraki*

* Okayama University,
3-1-1 Tshushimanaka, Kita-ku,
Okayama, Japan.

Published in: 2016 19th International Conference on Electrical Machines and Systems (ICEMS)

Extremum Co-Energy Principle for Analyzing AC Current Distribution in Parallel-Connected Wires of High Frequency Power Inductors

T. Shirakawa*, G. Yamasaki*, K. Umetani*, and E. Hiraki*
* Okayama University, 3-1-1 Tshushimanaka, Kita-ku, Okayama, Japan.

***Abstract*—Inductor winding is often composed as parallel-connected wires to suppress the copper loss. However, in high frequency inductors, the proximity effect can cause concentrated AC current distribution, hindering suppression of the copper loss. Therefore, optimization of the physical inductor structure requires predicting the AC current distribution. Although simulators are commonly employed for predicting the AC current distribution, simple analytical methods are also required for effective design or invention of the inductor structure with less copper loss. The purpose of this paper is to propose a novel analysis method of the AC current distribution in parallel-connected wires of high frequency inductors. The proposed method is based on a novel insight that the AC current is distributed to give an extremum of the magnetic co-energy contributed by the AC flux and the AC current under the given total AC current. Experiments are presented in this paper to verify the proposed method.**

***Index Terms*—AC current distribution, Magnetic co-energy, Inductor, Magnetic circuit.**

I. Introduction

The copper loss of power inductors are one of the major power loss in power converters. The copper loss is the Joule loss generated by the DC and AC current. As widely known, the copper loss can be effectively suppressed by designing sufficient wire cross-sectional area of the inductor winding. However, an extremely thick wire may cause difficulty in forming a winding because of its excessive stiffness. Therefore, the winding is often made as parallel-connected wires to increase the wire cross-sectional area [1]–[7].

Parallel-connected wires offer effective copper loss reduction particularly for the DC current, because the DC current distribution depends on the parasitic resistance. Generally, the current in the parallel-connected wires is distributed to achieve the same voltage drop among the wires. The DC component of the voltage drop equals to the parasitic resistance multiplied by the DC current. Therefore, the DC current is distributed uniformly among the parallel-connected wires of the same cross-sectional area, leading to effective loss reduction by the DC current.

On the other hand, parallel-connected wires do not necessarily contribute to effective copper loss reduction for the AC current [1]–[7]. The AC current causes the AC component of the voltage drop. The AC voltage drop equals to the AC impedance multiplied by the AC current. However, the AC impedance generally differs among the parallel-connected wires, even though the wire cross-sectional area is the same. The AC impedance is deeply affected by the leakage inductance and the complicated magnetic coupling among the wires. Therefore, the AC current is not necessarily distributed uniformly among the wires. This mechanism is widely known and referred to as the proximity effect.

The proximity effect tends to dominate the AC current distribution particularly in high frequency applications [1], [4], [6]–[8]. In this case, the parallel-connected wires may not effectively reduce the copper loss. This difficulty can be a severe issue particularly in inductors operated with large AC current at an extremely high frequency, because large inductor current tends to generate large copper loss.

In spite of this difficulty, recent progress of power electronics has given rise to a number of power converters whose inductors are operated with large AC current at a high frequency. Many of these converters are beneficial in miniaturization of passive components such as inductors and capacitors as well as reduction of switching loss. For example, critical conduction mode boot choppers [9]–[12] are widely utilized for the PFC converters. Besides, resonant LLC converters [13]–[16] are widely utilized for extremely high frequency applications. However, these converters tend to suffer from large copper loss caused by the large AC current. Therefore, effective suppression of the copper loss is intensely required.

The leakage inductance and the magnetic coupling, which cause the proximity effect, are intensely dependent on the physical structure of the core and the disposition of the wires [8], [17], [18]. Therefore, effective suppression of the copper loss may require design optimization of the inductor structure to achieve a uniform AC current distribution in the parallel-connected wires.

The AC current distribution of magnetic devices [4], [17], [18] has been analyzed and predicted commonly using FEM-based electromagnetic field analysis. However, numerical calculation may be inconvenient in practical inductor design because of its complicated analysis procedure as well as complicated model construction. Therefore, simple analytical methods may take an important role in practical inductor design.

In contradiction to the FEM analysis, few analytical methods have been known to predict the AC current distribution in parallel-connected wires of high frequency

inductors. For example, [3], [6], [7] proposed practical analytical methods with simple model construction. However, these methods may still suffer from comparatively complicated calculation process. For example, [3] utilized numerical calculation of the 1-dimensional magnetic field analysis. [6] partially utilized FEM analysis to determine the impedance of each wire. Besides, [7] modeled planar inductors as lumped circuit models. This method is beneficial because the circuit theory can be utilized for analysis of the AC current distribution. However, analysis by this method may suffer from complicated calculation because the lumped circuit models tend to have many ideal transformers, each of which represents a wire.

The purpose of this paper is to propose a simple analytical method that allows straightforward calculation based on the magnetic circuit model. This method can be utilized to predict the AC current distribution in high frequency inductors, in which the parasitic resistance can be approximated to have ignorable effect on the AC current distribution.

This proposed method is based on a novel insight proposed in this paper. According to this insight, the AC current is distributed to give an extremum of the magnetic co-energy [19][20] contributed by the AC flux and the AC current of the inductor under the condition of the given total AC current. Hereafter, this insight is referred to as the extremum co-energy principle.

The following discussion consists of 4 sections. Section II presents demonstration of the extremum co-energy principle. Section III presents the proposed analysis method of the AC current distribution. This section also presents basic examples of inductors with the EI cores. Section IV presents experiments on these examples to verify the proposed analysis method. Finally, section V gives conclusions.

II. Extremum co-energy principle

According to the extremum co-energy principle, the AC current in parallel-connected wires is distributed to give an extremum of the magnetic co-energy contributed by the AC flux and the AC current under the condition of the given total AC current. In this principle, the parasitic resistance of the wires is assumed to have ignorable effect on the AC current distribution. Therefore, the AC current distribution is rather dominantly determined by the leakage inductance and the magnetic coupling of the wires, as is often the cases in high frequency inductors.

The following discussion considers an inductor with parallel-connected n wires, as shown in Fig. 1. The current of wires 1, 2, …, n is denoted as i_1, i_2, …, i_n, respectively. We introduce the current vector $\mathbf{i}$ defined as $\mathbf{i}=[i_1, i_2, \ldots, i_n]^t$. The flux linkage of the wires is functions of $\mathbf{i}$. Therefore, we denote them as $\psi_1(\mathbf{i})$, $\psi_2(\mathbf{i})$, …, $\psi_n(\mathbf{i})$, respectively. In addition, we introduce the flux linkage vector $\boldsymbol{\psi}$ defined as $\boldsymbol{\psi}=[\psi_1, \psi_2, \ldots, \psi_n]^t$.

Then, the total magnetic co-energy E of this inductor can be expressed as

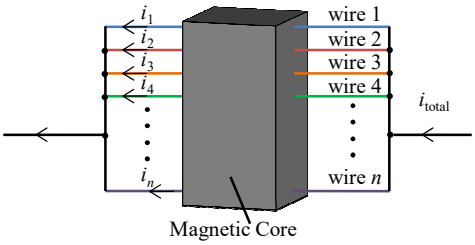

Fig. 1. Generalized inductor model with parallel connected wires.

$$E(\mathbf{i}) = \int_{\mathbf{0}}^{\mathbf{i}} \boldsymbol{\psi} \cdot d\mathbf{i} \,. \tag{1}$$

We regard current i_1, i_2, …, i_n as the sum of the DC current I_1, I_2, …, I_n and the AC current i_{ac1}, i_{ac2}, …, i_{acn}, respectively. We further regard the flux linkage ψ_1, ψ_2, …, ψ_n as the sum of the DC flux linkage ψ_{dc1}, ψ_{dc2}, …, ψ_{dcn} and the AC flux linkage ψ_{ac1}, ψ_{ac2}, …, ψ_{acn}, respectively. The DC current is assumed to be given. The DC flux linkage is also assumed to be given, because the DC flux linkage can be determined by the DC current.

We define the DC current vector $\mathbf{I}$ and the AC current vector $\mathbf{i}_{ac}$ as $\mathbf{I}=[I_1, I_2, \ldots, I_n]^t$ and $\mathbf{i}_{ac}=[i_{ac1}, i_{ac2}, \ldots, i_{acn}]^t$, respectively. Hence, $\mathbf{i}=\mathbf{I}+\mathbf{i}_{ac}$. We also define the DC flux linkage vector $\boldsymbol{\psi}_{dc}$ and the AC flux vector $\boldsymbol{\psi}_{ac}$ as $\boldsymbol{\psi}_{dc}=[\psi_{dc1}, \psi_{dc2}, \ldots, \psi_{dcn}]^t$ and $\boldsymbol{\psi}_{ac}=[\psi_{ac1}, \psi_{ac2}, \ldots, \psi_{acn}]^t$, respectively. Hence, $\boldsymbol{\psi}=\boldsymbol{\psi}_{dc}+\boldsymbol{\psi}_{ac}$.

Then, (1) can be rewritten as

$$\begin{aligned} E(\mathbf{I}, \mathbf{i}_{ac}) &= \int_{\mathbf{0}}^{\mathbf{I}} \boldsymbol{\psi}(\mathbf{i}) \cdot d\mathbf{i} + \int_{\mathbf{I}}^{\mathbf{I}+\mathbf{i}_{ac}} \boldsymbol{\psi}(\mathbf{i}) \cdot d\mathbf{i} \\ &= E_{dc}(\mathbf{I}) + \boldsymbol{\psi}_{dc} \cdot \mathbf{i}_{ac} + E_{ac}(\mathbf{I}, \mathbf{i}_{ac}), \end{aligned} \tag{2}$$

where E_{dc} is a function of $\mathbf{I}$ and E_{ac} is a function of $\mathbf{I}$ and $\mathbf{i}_{ac}$ defined as

$$\begin{aligned} E_{dc}(\mathbf{I}) &= \int_{\mathbf{0}}^{\mathbf{I}} \boldsymbol{\psi}(\mathbf{i}) \cdot d\mathbf{i}, \\ E_{ac}(\mathbf{I}, \mathbf{i}_{ac}) &= \int_{\mathbf{I}}^{\mathbf{I}+\mathbf{i}_{ac}} \boldsymbol{\psi}_{ac}(\mathbf{i}) \cdot d\mathbf{i} = \int_{\mathbf{0}}^{\mathbf{i}_{ac}} \boldsymbol{\psi}_{ac}(\mathbf{I}, \mathbf{i}_{ac}) \cdot d\mathbf{i}_{ac}. \end{aligned} \tag{3}$$

The condition of the given total AC inductor current can be expressed using i_{ac1}, i_{ac2}, …, i_{acn} as

$$i_{ac\_total} = \sum_{k=1}^{n} i_{ack}, \tag{4}$$

where k is the index of the wires, and i_{ac_total} is the given total AC current.

$E_{ac}(\mathbf{I}, \mathbf{i}_{ac})$ is the magnetic co-energy contributed by the AC flux and the AC current. Therefore, the extremum co-energy principle requires $E_{ac}(\mathbf{I}, \mathbf{i}_{ac})$ to take an extremum under the given total AC current i_{ac_total}.

Now, we seek for the solution of $\mathbf{i}_{ac}$ that gives an extremum of $E(\mathbf{I}, \mathbf{i}_{ac})$ under given i_{ac_total}. This solution can be obtained using the Lagrangian multiplier method. We introduce $E'(\mathbf{I}, \mathbf{i}_{ac}, \lambda)$ defined as

$$E'(\mathbf{I},\mathbf{i}_{\rm ac},\lambda)=E_{\rm ac}(\mathbf{I},\mathbf{i}_{\rm ac})+\lambda\left(i_{\rm ac\_total}-\sum_{k=1}^{n}i_{{\rm ac}k}\right), \tag{5}$$

where λ is the Lagrangian multiplier. Then, the solution of $\mathbf{i}_{\rm ac}$ must give an extremum of E'. Therefore, the solution meets the following requirement:

$$\frac{\partial E'}{\partial i_{\rm ac1}}=\frac{\partial E'}{\partial i_{\rm ac2}}=\cdots=\frac{\partial E'}{\partial i_{{\rm ac}n}}=0\,. \tag{6}$$

As a result, we obtain

$$\psi_{\rm ac1}=\psi_{\rm ac2}=\cdots=\psi_{{\rm ac}n}=\lambda\,. \tag{7}$$

Equation (7) indicates that the AC flux linkage in all the wires must be the same. This requirement is consistent with Kirchhoff's voltage law applied to the parallel-connected wires, because the time derivative of the AC flux linkage of a wire equals to the voltage induced in the wire, according to Faraday's law.

On the other hand, (4) corresponds to Kirchhoff's current law. Noting that $\psi_{\rm ac1}$, $\psi_{\rm ac2}$, …, $\psi_{{\rm ac}n}$ are the functions of $i_{\rm ac1}$, $i_{\rm ac2}$, …, $i_{{\rm ac}n}$, we can obtain the solution of $i_{\rm ac1}$, $i_{\rm ac2}$, …, $i_{{\rm ac}n}$ from (4) and (7). In fact, (4) and (7) suffice to determine all of $i_{\rm ac1}$, $i_{\rm ac2}$, …, $i_{{\rm ac}n}$ because (4) and (7) give n+1 equations of n+1 unknown parameters, i.e. $i_{\rm ac1}$, $i_{\rm ac2}$, …, $i_{{\rm ac}n}$, λ.

Consequently, the extremum co-energy principle is shown to be consistent with Kirchhoff's voltage law. This indicates the appropriateness of this principle. Furthermore, the extremum co-energy principle in combination with Kirchhoff's current law suffices to determine the AC current distribution in the parallel-connected wires.

III. Proposed Analysis Method of AC Current Distribution

A. Proposed Method

According to the extremum co-energy principle, we can determine the AC current distribution based on the magnetic circuit model. In the magnetic circuit model, the electromotive force follows Kirchhoff's voltage law; and, the flux follows the Kirchhoff's current law. Therefore, we can easily solve the flux passing through the reluctance using the circuit theory. As a result, we obtain the flux as functions of the wire current.

Then, the total magnetic co-energy contributed by the AC flux and the AC current can be obtained from this solution of the flux. For convenience, we neglect the magnetic saturation. Therefore, the reluctance is assumed to be constant. In this assumption, the AC flux linkage $\psi_{\rm ac1}$, $\psi_{\rm ac2}$, …, $\psi_{{\rm ac}n}$ is independent on the DC current **I**. Therefore, the magnetic co-energy contributed by the AC flux and the AC current equals to the total magnetic co-energy, when only AC current flows in the winding without DC current.

The total magnetic co-energy is the sum of the co-energy contributed by all the reluctance. As for the reluctance $\mathcal{R}$, through which only AC flux $\phi_{\rm ac}$ passes, the magnetic co-energy contributed by this reluctance can be expressed as $\mathcal{R}\phi_{\rm ac}^2/2$. Because the AC flux is a function of the AC current, the total magnetic co-energy at no DC current is a function of the AC current of the wires.

The solution of the current distribution must give an extremum of the magnetic co-energy at no DC current without changing the total AC current. This solution can be obtained as follows. Let $E(i_{\rm ac1}, i_{\rm ac2}, \ldots, i_{{\rm ac}n})$ be the total magnetic co-energy at no DC current as a function of the AC wire current $i_{\rm ac1}$, $i_{\rm ac2}$, …, $i_{{\rm ac}n}$; and, let $i_{\rm ac\_total}$ be the total AC current. We substitute the relation $i_{\rm ac\_total}=i_{\rm ac1}+i_{\rm ac2}+\ldots+i_{{\rm ac}n}$ into $E(i_{\rm ac1}, i_{\rm ac2}, \ldots, i_{{\rm ac}n})$ to eliminate one of the AC current. For convenience, we assume that $i_{\rm ac1}$ is eliminated. Then, the solution can be obtained as follows:

$$\frac{\partial E}{\partial i_{\rm ac2}}=\frac{\partial E}{\partial i_{\rm ac3}}=\cdots=\frac{\partial E}{\partial i_{{\rm ac}n}}=0\,. \tag{8}$$

The result gives n−1 equations of n−1 unknown parameters, i.e. $i_{\rm ac2}$, …, $i_{{\rm ac}n}$. Therefore, we can determine the AC current of all the wires.

B. Example 1

We consider an inductor with two parallel-connected wires wound on a pair of EI cores as shown in Fig. 2. The cores have gaps on the center and outer legs. The winding consists of two winding layers, each of which is formed by a wire and has the same number of turns N. We denote the wire that forms the winding layer closer to the gaps as wire 1; and we denote the other as wire 2.

For convenience, we assume that the magnetic cores have far greater permeability compared with the gaps and the leakage flux path; and therefore, we ignore the reluctance contributed by the magnetic cores. As a result, we obtain the magnetic circuit model of this inductor as shown in Fig. 3. Reluctance $\mathcal{R}_{\rm gap}$ is the reluctance of the flux path passing through the gaps, whereas $\mathcal{R}_{\rm leak}$ is the reluctance of the flux path through the area between the

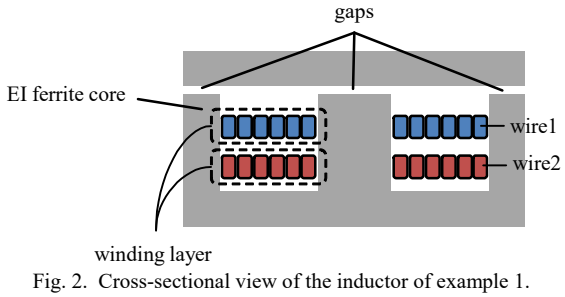

Fig. 2. Cross-sectional view of the inductor of example 1.

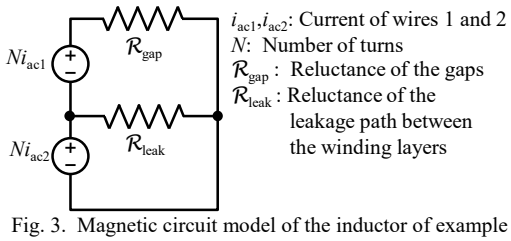

Fig. 3. Magnetic circuit model of the inductor of example 1.

winding layers. Current i_{ac1} and i_{ac2} are the AC current of wire 1 and 2, respectively.

The total magnetic co-energy E_{ex1} for Fig. 3 at no DC current can be expressed as

$$E_{ex1}=\frac{(Ni_{ac1}+Ni_{ac2})^2}{\mathcal{R}_{gap}}+\frac{N^2i_{ac2}^2}{\mathcal{R}_{leak}}, \tag{9}$$

We seek for the solution of i_{ac1} and i_{ac2} that gives an extremum of E_{ex1} under the condition of the same total AC current i_{ac_total}. Substituting this condition, i.e. $i_{ac\_total}=i_{ac1}+i_{ac2}$, into (9) to eliminate i_{ac1}, we obtain

$$E_{ex1}=\frac{N^2i_{ac\_total}^2}{\mathcal{R}_{gap}}+\frac{N^2i_{ac2}^2}{\mathcal{R}_{leak}}. \tag{10}$$

The result indicates that the magnetic co-energy takes an extremum at $i_{ac2}=0$. Therefore, all the current must flow in wire 1, which is the wire close to the gaps.

C. Example 2

Next, we analyze two other inductors, each of which has two parallel-connected wires wound on a pair of EI cores as shown in Fig. 4. The winding consists of four winding layers. Each wire forms two series-connected winding layers. In these examples, each winding layer has the same number of turns. However, the order of the winding layers differs between Fig. 4(a) and Fig. 4(b).

The magnetic circuit models of Fig. 4(a) and Fig. 4(b) are presented in Fig. 5(a) and Fig. 5(b), respectively. The total magnetic co-energy E_{ext2a} for Fig. 5(a) at no DC current is

$$\begin{aligned}E_{ex2a}&=\frac{(2Ni_{ac1}+2Ni_{ac2})^2}{\mathcal{R}_{gap}}+\frac{(Ni_{ac1}+2Ni_{ac2})^2}{\mathcal{R}_{leak}}\\&\quad+\frac{(Ni_{ac1}+Ni_{ac2})^2}{\mathcal{R}_{leak}}+\frac{Ni_{ac2}^2}{\mathcal{R}_{leak}}.\end{aligned} \tag{11}$$

We seek for the solution of i_{ac1} and i_{ac2} that gives an extremum of E_{ex2a} without changing the total inductor current i_{ac_total}. Substituting this condition, i.e. $i_{ac\_total}=i_{ac1}+i_{ac2}$, into (11) to eliminate i_{ac1}, we obtain

$$\begin{aligned}E_{ex2a}&=\frac{4N^2i_{ac\_total}^2}{\mathcal{R}_{gap}}+\frac{N^2i_{ac\_total}^2}{\mathcal{R}_{leak}}+\frac{(Ni_{ac\_total}+Ni_{ac2})^2}{\mathcal{R}_{leak}}+\frac{N^2i_{ac2}^2}{\mathcal{R}_{leak}}\\&=\frac{4N^2i_{ac\_total}^2}{\mathcal{R}_{gap}}+\frac{2N^2i_{ac\_total}^2}{\mathcal{R}_{leak}}+\frac{2N^2i_{ac\_total}i_{ac2}+2N^2i_{ac2}^2}{\mathcal{R}_{leak}}.\end{aligned} \tag{12}$$

According to the extremum co-energy principle, $\partial E_{ex2a}/\partial i_{ac2}$ must be zero. Therefore, we have

$$i_{ac1}=\frac{3}{2}i_{ac\_total},\quad i_{ac2}=-\frac{1}{2}i_{ac\_total}. \tag{13}$$

This result indicates that the inverse current flows in wire 2. Therefore, this disposition of the wires even increases the AC copper loss compared with the inductor with only one wires.

On the other hand, the total magnetic co-energy E_{ext2b} for Fig 5(b) is

$$\begin{aligned}E_{ex2b}&=\frac{(2Ni_{ac1}+2Ni_{ac2})^2}{\mathcal{R}_{gap}}+\frac{(Ni_{ac1}+2Ni_{ac2})^2}{\mathcal{R}_{leak}}\\&\quad+\frac{(Ni_{ac1}+Ni_{ac2})^2}{\mathcal{R}_{leak}}+\frac{N^2i_{ac1}^2}{\mathcal{R}_{leak}}.\end{aligned} \tag{14}$$

Substituting $i_{ac\_total}=i_{ac1}+i_{ac2}$ into (14) we obtain

$$\begin{aligned}E_{ex2b}&=\frac{4N^2i_{ac\_total}^2}{\mathcal{R}_{gap}}+\frac{N^2i_{ac\_total}^2}{\mathcal{R}_{leak}}+\frac{(2Ni_{ac\_total}-Ni_{ac1})^2}{\mathcal{R}_{leak}}+\frac{N^2i_{ac1}^2}{\mathcal{R}_{leak}}\\&=\frac{4N^2i_{ac\_total}^2}{\mathcal{R}_{gap}}+\frac{5N^2i_{ac\_total}^2}{\mathcal{R}_{leak}}+\frac{2N^2i_{ac1}^2-4N^2i_{ac\_total}i_{ac1}}{\mathcal{R}_{leak}}.\end{aligned} \tag{15}$$

Substituting (15) into $\partial E_{ex2b}/\partial i_{ac1}=0$, we have

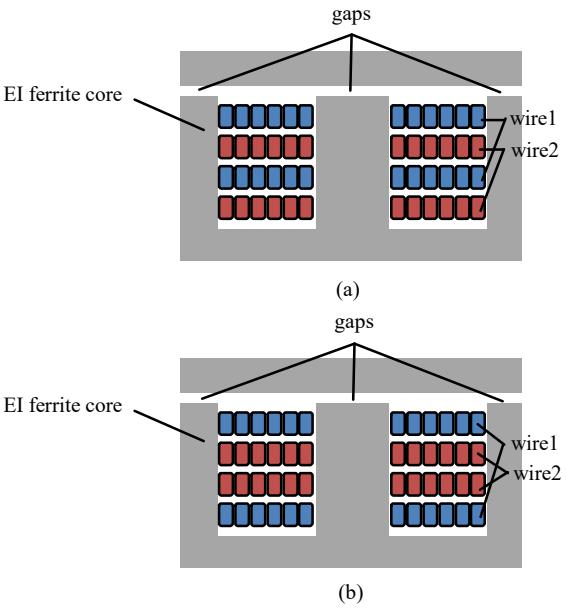

Fig. 4. Cross-sectional views of the inductor of example 2.

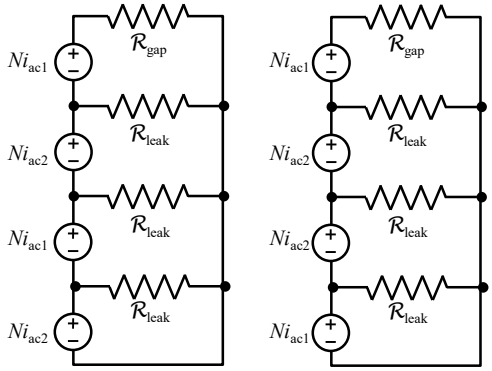

Fig. 4(a) Fig. 4(b)

i_{ac1},i_{ac2}: current of wires 1 and 2
N: Number of turns per layer
$\mathcal{R}_{gap}$: Reluctance of the gaps
$\mathcal{R}_{leak}$: Reluctance of the leakage path between neighboring winding layers

Fig. 5. Magnetic circuit models of the inductors of example 2.

$$i_{ac1} = i_{ac\_total}, \quad i_{ac2} = 0. \tag{16}$$

The result indicates that all the inductor current flows in wire 1. Therefore, Fig. 4(b) is more preferable than Fig. 4(a), although both of the inductor structures suffer from the concentration of the AC current.

As we have seen above, the proposed method can be applied to many cases in which even the value of the reluctance is unknown. This implies usefulness of the proposed method in practical inductor design.

IV. Experiment

Experiments were carried out to verify the proposed method. In the experiments, examples 1 and 2 shown in the previous section were evaluated.

A. Example 1

First, we evaluated example 1. Figure 6 shows the experimental inductor wound on a pair of EI cores. Specifications of the inductor are shown in Table I. The winding is composed as two parallel-connected wires of Litz wire (57 strands of ϕ0.1 wires). Each wire forms a winding layer of 7 turns. The core has the gaps of 1mm. The space between the winding layers is set at 1mm.

We applied the AC voltage of 300kHz to the experimental inductor. The total AC and DC inductor current was 0.50Arms and 0.0Arms, respectively. Then, the AC wire current was measured using Rogowski coils.

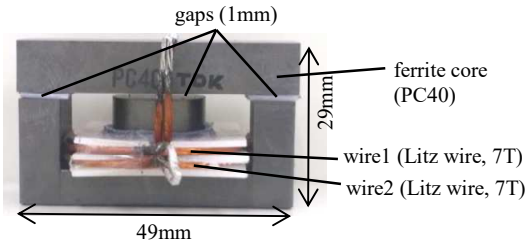

Fig. 6. Photograph of the experimental inductor of example 1.

TABLE I
SPECIFICATIONS OF THE INDUCTOR OF EXAMPLE 1

Inductance	14.65 μH
Litz wire (wire 1 and wire 2)	Sumitomo Electric Lz 1-FEIW-N ϕ0.1×57
Number of turns	7
Outer diameter of winding layers	35 mm
Inner diameter of winding layers	20 mm
Space between the winding layers	1 mm
Material of bobbin for coil	polyethylene
Size of E core	19×49×17 mm
Size of I core	9×49.5×14 mm
Mag. material	TDK PC40
gaps	1 mm
Material of gaps	polyethylene

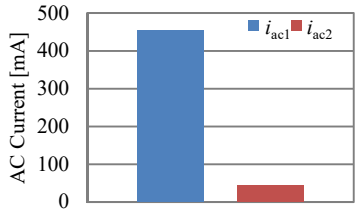

Fig. 7. Experimental result of the AC current distribution in the inductor of example 1.

The result is shown in Fig. 7. The result shows that almost all the AC current flows in wire 1. Therefore, the experiment verified the analysis for this example.

B. Example 2

Next, we evaluated example 2. Figure 8 shows two experimental inductors wound on a pair of EI cores. Specifications of the inductors are shown in Table II. The inductors have the winding of two parallel-connected wires of Litz wire (57 strands of ϕ0.1 wires), similarly as in example 1. Each wire forms two winding layers of 6 turns. The core has the gaps of 1mm. The spaces between the winding layers are set at 0.5mm.

First, we evaluated the AC current distribution in the parallel-connected wires. We again applied the AC voltage of 100kHz to the inductors. The total AC and DC current were set at 1.0Arms and 0.0Arms, respectively. Figure 9 shows the result. As for Fig. 8(a), the inverse current was successfully found in wire 2, although the amplitude of the inverse current was slightly smaller than the theory. Furthermore, almost all the AC current flows in wire 1 in Fig. 8(b), which is also consistent with the theory.

In addition, we measured the AC resistance of the experimental inductors at 100kHz with an LCR-meter.

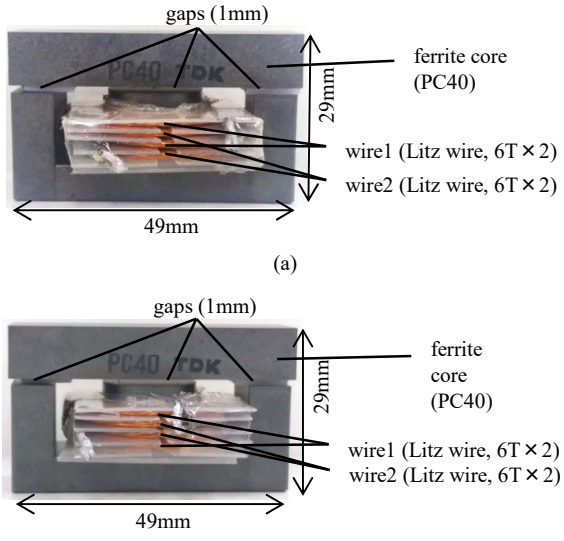

Fig. 8. Photographs of the experimental inductors of example 2.

TABLE II
SPECIFICATIONS OF THE INDUCTOR OF EXAMPLE 2

Inductance of Fig. 8(a)	34.57 μH
Inductance of Fig. 8(b)	35.14 μH
Litz wire (wire 1 and wire 2)	Sumitomo Electric Lz 1-FEIW-N ϕ0.1×57
Number of turns per layer	6
Outer diameter of winding layers	33 mm
Inner diameter of winding layers	20 mm
Space between the winding layers	0.5 mm
Material of bobbin for coil	polyethylene
Size of E core	19×49×17 mm
Size of I core	9×49.5×14 mm
Mag. material	TDK PC40
gaps	1 mm
Material of gaps	polyethylene

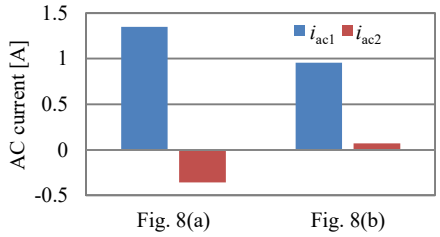

Fig. 9. Experimental results of the AC current distribution in the inductors of example 2.

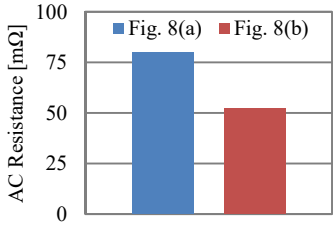

Fig. 10. Experimental results of the AC resistance in the inductors of example 2.

The result is shown in Fig. 10. The result revealed that Fig. 8(b) reduced the AC power loss compared with Fig. 8(a), contributed by reduction of the inverse current.

Consequently, we concluded that the experiment verified the proposed method.

V. Conclusions

Parallel-connected wires are commonly utilized for the inductor winding to suppress the copper loss. However, the proximity effect can cause concentration of AC current in a wire, hindering effective suppression of the AC copper loss. Therefore, predicting the AC current distribution is required to optimize the inductor structure. In order to provide a straightforward method to predict the AC current distribution, this paper proposed a novel analysis method based on the extremum co-energy principle. This paper presented two examples, in which the AC current distribution is analyzed using the proposed method. The results are experimentally verified, supporting appropriateness of the proposed method.

References

[1] R. Prieto, J. A. Cobos, O. Garcia, P. Alou, and J. Uceda, "Using parallel windings in planar magnetic components," *Proc. IEEE Power Electron. Specialist Conf.* (PESC2001), Vancouver (Canada), Jun. 2001, vol. 4, pp. 2055-2060.

[2] Y. Hu, J. Guan, X. Bai, and W. Chen, "Problems of paralleling windings for planar transformers and solutions," *Proc. IEEE Power Electron. Specialist Conf.* (PESC2002), vol. 2, pp. 597-601.

[3] W. Chen, Y. Yan, Y. Hu, and Q. Lu, "Model and design of pcb parallel winding for planar transformer," *IEEE Trans. Magn.*, vol. 39, no. 5, pp. 3202-3204, Sept. 2003.

[4] D. Fu, F. C. Lee, and S. Wang, "Investigation on transformer design of high frequency high efficiency DC-DC converters," *Proc. Appl. Power Electron. Conf. Expo.* (APEC2010), Palm Springs (CA, USA), Feb. 2010, pp. 940-947.

[5] X. Margueron, A. Besri, Y. Lembeye, and J. P. Keradec, "Current sharing between parallel turns of a planar transformer: prediction and improvement using a circuit simulation software," *IEEE Trans. Ind. Appl.*, vol. 46, no. 3, pp. 1064-1071, May/Jun. 2010.

[6] R. Prieto, R. Asensi, and J.A. Cobos, "Selection of the appropriate winding setup in planar inductors with parallel windings," *Proc. IEEE Energy Conversion Congr. Expo.* (ECCE2010), Atlanta (GA, USA), Sept. 2010, pp. 4599-4604.

[7] M. Chen, M. Araghchini, K. K. Afridi, J. H. Lang, C. R. Sullivan, and D. J. Perreault, "A systematic approach to modeling impedances and current distribution in planar magnetics," *IEEE Trans. Power Electron.*, vol. 31, no. 1, pp. 560-580, Jan. 2016.

[8] J. D. van Wyk Jr.,W. A. Cronje, J. D. vanWyk, C. K. Campbell, and P. J. Wolmarans, "Power electronic interconnects: skin- and proximity effect-based frequency selective multipath propagation," *IEEE Trans. Power Electron.*, vol. 20, no. 3, pp. 600-610, May 2005.

[9] E. Finnansyah, S. Tomioka, S. Abel, M. Shoyama, and T. Ninomiya, "A critical-conduction-mode bridgeless interleaved boost power factor correction," *Proc. IEEE Intl. Telecommunications Energy Conf.* (INTELEC2009), Incheon (Korea), Oct. 2009, pp. 1-5.

[10] J. C. Hernandez, L. P. Petersen, M. A. E. Andersen, "Characterization and evaluation of 600 v range devices for active power factor correction in boundary and continuous conduction modes," *Proc. Appl. Power Electron. Conf. Expo.* (APEC2015), Charlotte (NC, USA), Mar. 2015, pp. 1911-1916.

[11] J.-W. Kim and G.-W. Moon, "Minimizing effect of input filter capacitor in a digital boundary conduction mode power factor corrector based on time-domain analysis," *IEEE Trans. Power Electron.*, vol. 31, no. 6, pp. 3827-3836, May 2016.

[12] Z. Liu, Z. Huang, F. C. Lee, and Q. Li, "Digital-based interleaving control for GaN-based MHz CRM totem-pole PFC," *Proc. Appl. Power Electron. Conf. Expo.* (APEC2016), Long Beach (CA, USA), Mar. 2016, pp. 1847-1852.

[13] G. Ivensky, S. Bronshtein, and A. Abramovitz, "Approximate analysis of resonant LLC DC-DC converter," *IEEE Trans. Power Electron.*, vol. 26, no. 11, pp. 3274-3284, Nov. 2011.

[14] G. Yang, P. Dubus, and D. Sadarnac, "Double-phase high-efficiency, wide load range high-voltage/low-voltage LLC DC/DC converter for electric/hybrid vehicles," *IEEE Trans. Power Electron.*, vol. 30, no. 4, pp. 1876-1886, Apr. 2015.

[15] H. Li and Z. Jiang, "On automatic resonant frequency tracking in LLC series resonant converter based on zero-current duration time of secondary diode," *IEEE Trans. Power Electron.*, vol. 31, no. 7, pp. 4956-4962, Jul. 2016.

[16] W. Zhang, F. Wang, D. J. Costinett, L. M. Tolbert, and B. J. Blalock, "Investigation of gallium nitride devices in high frequency LLC resonant converter," *IEEE Trans. Power Electron.*, vol. PP, no. 99.

[17] Y Suzuki, I. Hasegawa, S. Sakabe, T. Yamada, "Effective electromagnetic field analysis using finite element method for high frequency transformers with Litz-wire," *Proc. IEEE Intl. Conf. Elect. Mach. Syst.* (ICEMS2008), Wuhan (China), Oct. 2008, pp. 4388-4393.

[18] V. Nabaei, S. A. Mousavi, K. Miralikhani, and H. Mohseni, "Balancing current distribution in parallel windings of furnace transformers using the genetic algorithm," *IEEE Trans. Magn.*, vol. 46, no. 2, pp. 626-629, Feb. 2010.

[19] R. Krishnan, *Switched reluctance motor drives*, Boca Raton, FL, USA: CRC Press, 2000, pp. 3–7.

[20] T. J. E. Miller, *Electronic control of switched reluctance machines*, Oxford, U. K.: Newns, 2001, pp. 43–45.